Pharm Res (2015) 32:2029–2037
DOI 10.1007/s11095-014-1595-9

RESEARCH PAPER

Physiology-Based Pharmacokinetics of Caspofungin for Adults and Paediatrics

Felix Stader • Gudrun Wuerthwein • Andreas H. Groll • Joerg-Janne Vehreschild • Oliver A. Cornely • Georg Hempel

Received: 18 September 2014 / Accepted: 3 December 2014 / Published online: 19 December 2014

ABSTRACT

Purpose Caspofungin (CAS) is an antifungal agent for intravenous application in adults and children. Our aim was the development and validation of a physiology-based pharmacokinetic (PBPK) model in order to predict the pharmacokinetics in different patient populations, particularly in paediatrics.

Methods A PBPK model for adults was built and validated with raw data of the two clinical trials CASLAMB and CASMTD. Afterwards, the model was scaled for paediatric patients under the consideration of known biochemical differences between adults and paediatrics.

Results The simulated results of the PBPK model were in good agreement with the observed values of the CASLAMB and CASMTD trial. Patients of the CASLAMB trial received CAS in combination with cyclosporine A (CsA), which leads to an increased AUC_{0-24h} of CAS hypothetically due to an inhibition of the hepatic transport protein OATP1B1 by CsA. However, there was no difference in the transport rate of OATP1B1 between CASLAMB and CASMTD patients in the PBPK model, suggesting that CsA might not influence OATP1B1. Furthermore, the model was able to sufficiently predict the pharmacokinetics of paediatric patients compared to published data.

Conclusion The final PBPK model of CAS without individualized parameter is able to predict the pharmacokinetics in different patient populations correctly. Thus, the model provides a basis for investigators to choose doses and sampling times for special populations such as infants and small children.

KEY WORDS caspofungin · paediatrics · physiology-based pharmacokinetic model · PK-Sim®

ABBREVIATION

AUC	Area under the curve
CAS	Caspofungin
CI	Confidence interval

F. Stader · G. Hempel (✉)
Institute of Pharmaceutical and Medical Chemistry - Department of Clinical Pharmacy, Westfaelische Wilhelms-University Muenster Corrensstraße 48, 48149 Muenster, Germany
e-mail: hempege@uni-muenster.de

F. Stader
e-mail: f_stad01@uni-muenster.de

F. Stader
e-mail: felix.stader@certara.com

G. Wuerthwein
Centre for Clinical Trials (ZKS, BMBF 01KN1105), Muenster, University Hospital Muenster Von-Esmarch-Straße 62, 48149 Muenster, Germany
e-mail: gudrun.wuerthwein@ukmuenster.de

A. H. Groll
Centre for Bone Marrow Transplantation and Department of Paediatric Haematology / Oncology, University Hospital Muenster Albert-Schweitzer-Campus 1, 48149 Muenster, Germany
e-mail: grollan@ukmuenster.de

J.-J. Vehreschild
Department I of Internal Medicine, German Centre for Infection Research, partner site Bonn-Cologne, University of Cologne Kerpener Straße 62, 50937 Cologne, Germany
e-mail: janne.vehreschild@ctuc.de

O. A. Cornely
Department I of Internal Medicine, Cologne Excellence Cluster on Cellular Stress Responses in Aging-Associated Diseases (CECAD), Clinical Trials Centre Cologne, ZKS Köln, BMBF 01KN1106, Center for Integrated Oncology CIO KölnBonn, German Centre for Infection Research, University of Cologne Kerpener Straße 62, 50937 Cologne, Germany
e-mail: oliver.cornely@uk-koeln.de

Present Address:
F. Stader
Simcyp Limited (a Certara Company), Blades Enterprise Centre John Street, S2 4SU Sheffield, UK

CL_H	Hepatic clearance
CL_{int}	Hepatic intrinsic clearance
fu	Fraction unbound
GEOM	Geometric mean
GOF	Goodness of fit
HTK	Haematocrit
i.v.	Intravenous
$K_{rbc,\ u}$	Partition coefficient of the unbound fraction into the red blood cells
LAMB	Liposomal Amphotericin B
OATP	Organic anion transporting polypeptide
PBPK	Physiology based pharmacokinetic
PE	Prediction error
POP-PK	Population pharmacokinetic
Q_H	Hepatic blood flow

INTRODUCTION

Caspofungin (CAS) is an intravenous (i.v.) echinocandin. The compound exhibits useful clinical efficacy against the two most common pathogenic fungi, *Candida* spp. and *Aspergillus* spp. [1–5] and has demonstrated excellent safety and tolerability [6]. CAS is a non-competitive inhibitor of the β-1,3-D-glucan-synthase [7], an enzyme complex catalysing the polymerisation of uridin-diphosphate-glucose to β-1,3-D-glucans [8] in many pathogenic fungi. β-1,3-D-glucan is an essential component of the cell wall and loss leads to cell lyses in *Candida* spp. and to morphological damage of hyphae in *Aspergillus* spp. [9]. CAS has been approved by the FDA, the EMA and other regulatory authorities for treatment of invasive aspergillosis, invasive candidiasis and oesophageal candidiasis or as empirical therapy for presumed fungal infections in patients with persistent fever and neutropenia [10]. The efficacy, safety and pharmacokinetics in paediatric patients are similar to adults, if dosage regime in paediatric patients is based on body surface area [11]. The pharmacokinetic of CAS is consistent between animals and humans [12, 13]. Similar to other echinocandins, CAS is highly bound to plasma proteins and displays a triphasic area under the curve (AUC). Immediately after the infusion of CAS, there occurs a short α-phase with a half-life of one to two hours. The log linear, dominant β-phase, which represents 80% of the total AUC, succeeded after the α-phase. 48 h after the infusion started, there is an additional γ-phase [13–15]. CAS is well distributed into tissues except heart and brain [13]. The intake into the liver is a biphasic process with a fast, reversible binding to the surface of hepatocytes and a slow transport through the active organic anion transporting polypeptide 1B1 (OATP1B1) [16]. Hydrolysis and *N*-acetylation degrade the compound slowly, primarily in the liver [17]. Total plasma clearance is 10 to 12 ml/min [13, 18] and the main elimination route is probably hepatic, because only one to two per cent of the antifungal agent is cleared renal [17]. There is an uncertainty in literature whether CAS exhibits linear [19] or nonlinear pharmacokinetics [15]. CAS is neither a substrate nor an inhibitor of cytochrome-P-450 enzymes or P-glycoprotein and there are no clinically relevant interactions through these systems [17, 20]. If CAS is administered together with the immunosuppressive calcineurin inhibitor cyclosporine (CsA), the AUC of CAS will raise up to 30% while the concentration of CsA will remain unchanged [20].

Physiology-based pharmacokinetic (PBPK) modelling describes physical, chemical and physiological processes of drug absorption, distribution, metabolism and elimination mathematically [21]. PBPK predicts the pharmacokinetics of a drug based on physiological and drug-specific data, such as physicochemical properties, clearance, distribution into tissues and metabolism or active transport [21–23]. A difference compared to classical pharmacokinetic models is that compartments represent tissues and organs with their physiological volume and blood flow rates. The different compartments are linked by arteries and veins, which are pooled in the lung [23, 24]. Organs and tissues are further divided into the subcompartments plasma, red blood cells, interstitial volume and cytosol [25]. Diffusion of a drug into an organ can be limited by blood flow (well-stirred models) or by permeability. The distribution of a drug is described by mass balance equations [23, 24]. PBPK models are used to predict the pharmacokinetics by scaling animal data to humans [26] or by scaling data from healthy volunteers to different populations such as paediatric patients [27].

The aim of this investigation was to build and validate a PBPK model with the ability to simulate the pharmacokinetics of CAS in different adult patient populations. Furthermore, the PBPK model was used to predict the pharmacokinetics in paediatric patients, because there is a paucity of clinical data, especially in infants and small children. In order to evaluate the predictive value of the method, we compared the results with published pharmacokinetic parameters from paediatric patients.

MATERIAL AND METHODS

Pharmacokinetic Data from Adults

Raw data of 35 patients of the CASLAMB trial [28], receiving CAS, were used as the development dataset. CASLAMB was an open prospective randomized multicentre phase II trial to investigate the safety and pharmacokinetics of CAS (18 patients), liposomal amphotericin B (LAMB; 20 patients) and the combination of both (17 patients) in allogeneic haematopoietic stem cell recipients. CAS was administered once daily as an i.v. infusion over 60 min at a dose of 70 mg on day 1 followed by 50 mg until the end of therapy. Pharmacokinetic sampling was performed

serially on day 1 and 4 of therapy at specific time intervals (0.5 to 1.5 h, 1.5 to 3 h, 3 to 5 h, 5 to 11 h, and 22 to 23 h after the infusion started) and afterwards twice a week. The 35 patients (15 female / 20 male), receiving CAS or the combination of CAS and LAMB, had a median age (range) of 45 years (20–61), a median body weight of 75 kg (54–99) and a median body height of 174 cm (151–191). All patients received co-medication with an individual dose of CsA, which interacts with CAS [28].

Raw data of 46 patients of the CASMTD trial [29] were used to validate the adult model. CASMTD was a formal phase II dose escalation trial in patients with invasive aspergillosis. CAS was administered once daily as an i.v. infusion over 120 min at 70 mg (9 patients), 100 mg (8 patients), 150 mg (9 patients) and 200 mg (20 patients). Pharmacokinetic sampling was performed serially on day 1 (2, 3, 5–7 and 24 h after the infusion started) and peak (at the end of infusion) and trough levels (immediately before the next infusion started) were collected on day 4, 7, 14 and 28. The 46 patients included (21 female and 25 male) had a median age (range) of 61 years (18–74), a median body weight of 76 kg (43–104) and a median body height of 173 cm (153–189) [29].

Development of the Basic PBPK Model

For all simulations PK-Sim® version 5.1.5 and MoBi® version 3.1 (Bayer Technology Services GmbH, Leverkusen, Germany) were used, which implement a whole-body PBPK model. The lipophilicity of CAS was inserted with a log *p* value of 0 and the molecular weight of CAS was 1093.31 g/mol [30]. The measurement of the fraction unbound (fu) in human yielded 3.5% [13].

Simulation of Metabolism and Excretion

Hepatic plasma clearance in the model was 0.15 ml/min/kg and the renal clearance was 0.0018 ml/min/kg [13]. The active transporter OATP1B1 was built into the basolateral membrane of hepatocytes with a relative expression of 0.252 [31]. There are no available literature data for the kinetic parameters of OATP1B1 for CAS transport [16]. For K_M, a value of 100 μmol/l was chosen, because other drugs with a slow transport rate have been shown to have K_M values less than 85 μmol/l [32]. K_{cat}, which is defined as the quotient of V_{max} and the transporter concentration, was parameterised, because OATP1B1 is a highly polymorphic transporter. It is yet unclear, if the rate of expression (and hence the concentration of the transporter) or the molecule itself is influenced by polymorphisms [33, 34]. For the parameterisation of k_{cat}, the Nelder-Mead-Algorithms in the Matlab®-Toolbox for MoBi® was used. The individual k_{cat} values were taken for the individualised model and the median of the CASLAMB patients was used for the general model, as different genotypes of OATP1B1 don't have a Gaussian distribution in the population [35].

The method described by Rodgers & Rowland [36, 37] was the best-implemented partition coefficient method in PK-Sim®, which had the ability to predict the tissue distribution. The interstitial : plasma partition coefficient was raised by a factor 1.8 to obtain a better prediction of the α-phase of CAS. The endothelial permeability was decreased to $1.5*10^{-3}$ cm/min with the exception of the liver (endothelial permeability: 100 cm/min), since a fast reversible absorption on the cell surface of hepatocytes has been described *in vitro* [16].

Pharmacokinetic Simulations of Paediatric Patients

Pharmacokinetic variability of paediatrics was assessed by creating virtual populations aged 1 day, 1 month, 2 and 3 month up to 23 months and 2 years, 3 and 4 years up to 18 years. Physiological data was used from the ICRP database for Europeans [38]. The age in one population was the same for all virtual individuals. The body weight and body height of one population ranged from the median value of the previous age group to the next age group. Paediatric patients up to 3 month received 25 mg/m^2/day and those up to 18 years a dose of 70 mg/m^2 on day 1 and 50 mg/m^2/day until the end of therapy.

Age-Dependent Scaling of PBPK Model Parameters

Protein Binding

The protein binding for paediatric patients was estimated using the equations of McNamara & Alcorn [39].

Clearance

Before scaling the clearance of CAS from adults to paediatric patients, it was assumed that:

1. Pathways of elimination are the same in adults and children (the main elimination route for CAS is assumed to be hepatic)
2. Well-stirred conditions hold true in children (hepatic uptake of CAS is limited by blood flow not by permeability)
3. Active transport processes follow first order kinetics (concentrations are within linear range—OATP1B1 is not saturable)

Hepatic clearance (CL_H) was scaled according to Eq. 1 [27]:

$$CL_{H,\,child} = \frac{Q_{H,\,child} \times f_{u,\,child} \times CL_{int,\,child}}{Q_{H,\,child} + \left(\frac{f_{u,\,child} \times CL_{int,\,child}}{1 + \left(HTK_{child} \times \left(f_{u,\,child} \times K_{rbc,\,u} - 1 \right) \right)} \right)} \quad (1)$$

where Q_H is the hepatic blood flow, CL_{int} is the intrinsic clearance, HTK is the haematocrit and $K_{rbc,\ u}$ is the partition coefficient of the fraction unbound into the red blood cells. $K_{rbc,\ u}$ is assumed to be constant between adults and children and has got a value of 12.8.

Renal clearance (CL_R) was estimated according to Eqs. 2 and 3 [13, 27]:

$$CL_{R,\ child} = CL_{GFR,\ child} \times F_{RT} \quad (2)$$

$$CL_{GFR,\ child} = \frac{GFR_{child}}{GFR_{adult}} \times \frac{f_{u,\ child}}{f_{u,\ adult}} \times CL_{GFR,\ adult} \quad (3)$$

where CL_{GFR} is the clearance due to glomerular filtration (GFR) and F_{RT} is the factor of tubular reabsorption (for CAS F_{RT} is 4% [13]). The values of GFR_{child} were taken from Rubin *et al.* [40] and the GFR_{adult} was assumed to be 120 ml/min. Based on a GFR_{adult} of 120 ml/min and a plasma fu of 3.5%, $CL_{GFR,\ \mathrm{adult}}$ is 4.2 ml/min.

OATP1B1

Until now there is no information about the ontogeny of OATP1B1 available. Therefore, the kinetic data from adults were taken for paediatric patients.

Evaluation of PBPK Models

The evaluation of PBPK models was carried out by visual comparison between the predicted data of PK-Sim® and the observed data of the CASLAMB and the CASMTD trial. Goodness of fit (GOF) plots were performed to analyse the accuracy between simulated and observed data. The prediction error (PE) was estimated according to Eq. 4.

$$PE = \frac{simulated - observed}{observed} \times 100 \quad (4)$$

Doses linearity was analysed using the doses escalation trial CASMTD, because there is an uncertainty in literature whether CAS exhibits linear [19] or nonlinear pharmacokinetics [15]. The analysis was carried out with the model that includes the individualised k_{cat} values (individualised model). At first, the simulated concentration-time-curve and the plasma fu were divided by doses and it was visually analysed if a superposition occurred. Second, the geometric mean (GEOM) for peak and trough levels and AUC_{0-24h} of the particular doses cohort were plotted against doses and the correlation coefficient was estimated. If the correlation coefficient was one, doses linearity would be expected. Clearance and half-life were also plotted against doses and both should be independent of doses. Third, changes in trough levels were analysed to evaluate the time at which virtual patients entered steady state. Finally, the accumulation ratio of trough levels based on day 1 and day 14 were evaluated by calculating the geometric mean ratio (day 14 / day 1) with 95 confidence interval (CI).

In the literature, it is discussed if CsA inhibits the OATP1B1 transport, especially for statins [20, 41, 42]. Therefore, it was investigated, if the parameterised k_{cat} values of OATP1B1 for CAS transport and hence the amount of CAS transported per time unit (transport rate) were different between CASLAMB (with CsA) and CASMTD patients (without immunosuppression by CsA). The general model was also used to predict the pharmacokinetics of published healthy volunteers [13, 15, 18] and k_{cat} was estimated with the same method as for CASLAMB and CASMTD patients. K_{cat} values of all three analyses were compared by using a bilateral, unpaired Wilcoxon-Test in the software R® 3.0 [43]. Due to the hypothetical inhibition of OATP1B1 by CsA, higher k_{cat} values are expected in CASMTD patients and in healthy volunteers in comparison to CASLAMB patients receiving CsA.

Finally, the predicted peak and trough levels as well as the AUC_{0-24h} in virtual paediatric patients were compared with published data from paediatric trials by calculating the GEOM with 95% CI. Paediatric patients were classified in infants (0 to 3 months), toddlers (3 to 23 months), children (2 to 11 years) and adolescents (12 to 18 years). Pharmacokinetic data were obtained as published by Saez-Llorens *et al.* [44] for premature infants, Neely *et al.* [45] for toddlers and Walsh *et al.* [11] for children and adolescents. All pharmacokinetic parameters were analysed at steady-state.

RESULTS

Development Dataset

After OATP1B1 was built into the virtual liver of patients and the median of individualised k_{cat} from the CASLAMB trial was entered with 13.1 min^{-1}, the predicted concentration-time-curve was in accordance to the observed mean values of CASLAMB patients (Fig. 1a). All aberrations were within the SD of the observed values. The GOF plot showed a good accuracy between predicted and observed data (Fig. 1b). 80 of the CAS values were within a PE of ±30 and 97% within ±50% (Data not shown). The predicted GEOM of the total clearance in the PBPK model was 0.474 L/h (95% CI: 0.413; 0.534), which is in accordance with the clearance of 0.462 L/h (95 CI: 0.423; 0.503) from a population pharmacokinetic (POP-PK) analysis of the same data [46].

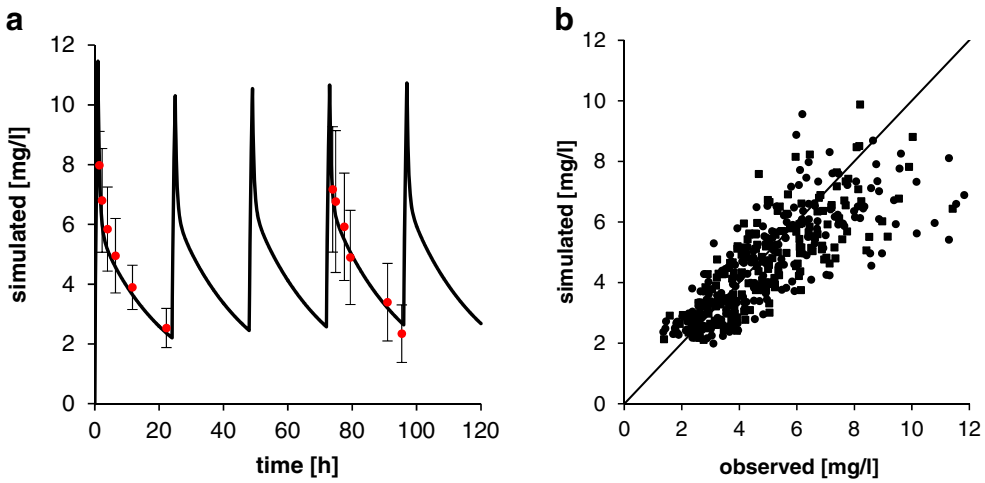

Fig. 1 Simulation results of the CASLAMB trial [28]. (**a**) shows the predicted (*black line*) and observed (*red dots*) data of the CASLAMB trial. Observed data from pharmacokinetic sampling on days 1 and 4 of the 35 patients were pooled as mean ± SD. (**b**) shows the GOF-Plot of these patients.

Validation Dataset

The final PBPK model of CAS without individualised parameters was able to predict the observed concentration-time profile for all doses cohorts (70 mg, 100 mg, 150 mg and 200 mg) of the CASMTD patients correctly (Fig. 2a–d). Simulated peak levels appear to be underestimated by 20% for all doses levels, but they were within the range of the observed SD. The GOF plot showed a sufficient accuracy between predicted and observed data (Fig. 3). Only the simulated peak levels seemed to be underestimated in PK-Sim®. 79% of the CASMTD values were within a PE of ±30 and 95% within ±50% (Data not shown). In summary, the model was able to predict the pharmacokinetics in a different adult patient population with different CAS doses correctly. The GEOM of plasma clearance calculated from the PBPK model was 0.419 L/h (95% CI: 0.264; 0.529) *vs.* 0.401 L/h (95% CI: 0.372; 0457) from the POP-PK model of the same data [19].

Dose Linearity

CASMTD was a classical dose escalation trial, thereby suitable to analyse linear or nonlinear pharmacokinetics. Both the simulated concentration-time-curve in plasma and the predicted plasma fu

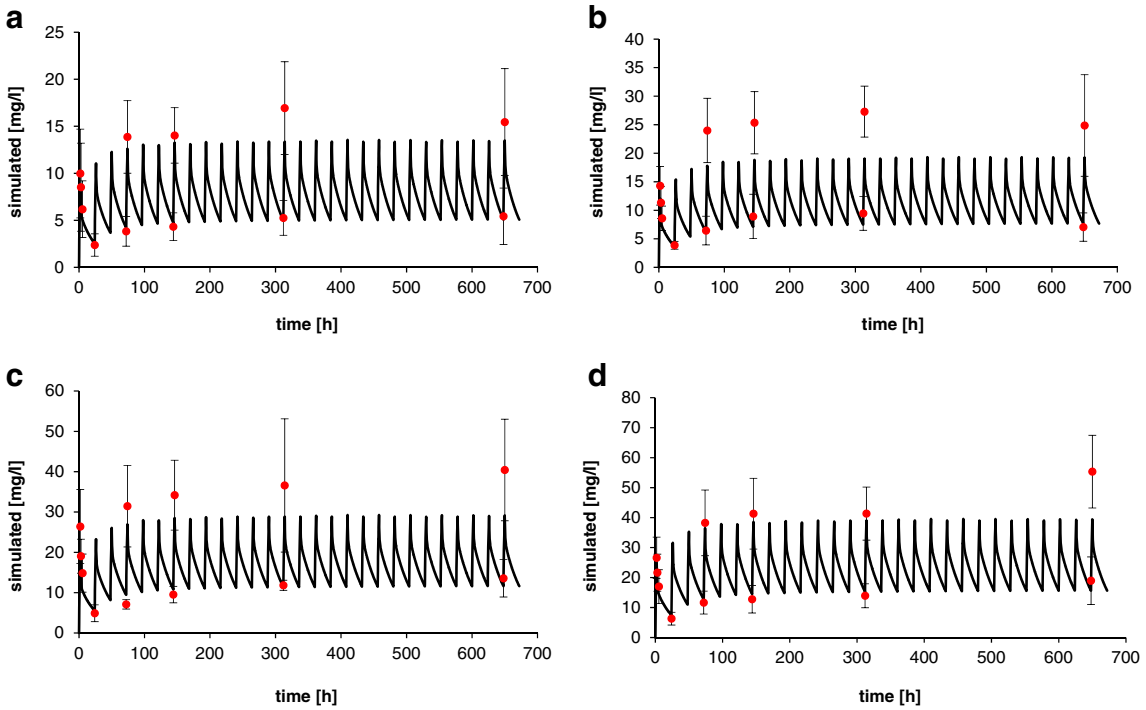

Fig. 2 Simulation results of the 70 mg (**a**), 100 mg (**b**), 150 mg (**c**) and 200 mg (2D) doses cohort of the MTD trial [29]. *Red dots* are the mean observed data ± SD.

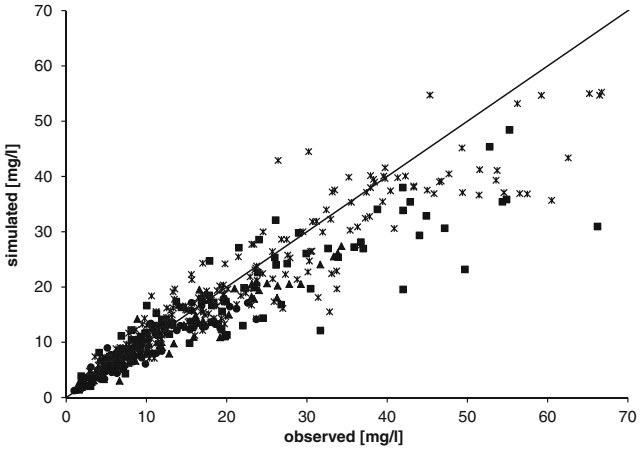

Fig. 3 GOF plot of the MTD trial [29]. 70 mg doses cohort: $n=9$, *dots*; 100 mg doses cohort: $n=8$, *triangle*; 150 mg doses cohort: $n=9$, *quadrats*; 200 mg doses cohort: $n=20$, *stars*.

(data not shown) were superimposable. Notably, the simulated concentration-time-profile but not the plasma fu of the 150 mg doses cohort was 20 to 30% lower than the profiles from the other dose cohorts. Predicted peak and trough levels as well as the AUC_{0-24h} were proportional to doses and in addition clearance and half-life showed dose independency (data not shown). Time to reach steady state conditions was also independent of dose level in the simulation. In the PBPK model nearly 50% of the patient from the CASMTD trial reached steady state at day 4 (70 mg cohort: $n=5$; 100 mg cohort: $n=4$; 150 mg cohort: $n=4$ and 200 mg cohort: $n=13$). Of note, some patients did not even reach steady state until day 28 in the PK-Sim® simulation (70 mg cohort: $n=2$; 100 mg cohort: $n=2$; 150 mg cohort: $n=4$ and 200 mg cohort: $n=2$). The accumulation of trough levels did not depend on doses. GEOM of the accumulation ratio (day 14 / day 1) of trough levels were 1.91 (95% CI: 1.26; 2.81), 2.10 (95% CI 1.84; 2.55); 2.59 (95% CI: 1.63; 3.80) and 1.63 (95% CI: 1.19; 2.03) for the 70 mg, 100 mg, 150 mg and 200 mg cohort, respectively. Taken together, these results indicate linear pharmacokinetics of CAS over the investigated dose range.

CsA Interaction

The parameterisation of k_{cat} for the OATP1B1 transport of CAS was carried out in the Matlab®-Toolbox for MoBi®, using the Nelder-Mead algorithm. In the literature, it is discussed if CsA inhibits OATP1B1 leading to higher AUC values of other drugs, particularly of statins [20, 41, 42]. Therefore, the predicted amount of CAS transported per time unit from the CASLAMB trial (with CsA) and the CASMTD study (without immunosuppression by CsA) were compared. Surprisingly, there was no significant difference in the median values of k_{cat} for CASLAMB patients with a value of 13.1 min^{-1} (95% CI: 7.6; 18.0) and CASMTD patients with a value of 11.7 min^{-1} (95% CI: 7.0; 20.9). The general model was used to predict the pharmacokinetics in healthy volunteers [13, 15, 18] and the k_{cat} value of the OATP1B1 was parameterised with the same method. The median predicted k_{cat} value in Matlab® for healthy volunteers was 20.1 min^{-1} (95% CI: 17.2; 23.9). Thus, the transport rate of CAS in CASLAMB- and CASMTD patients was reduced by up to 40% compared to healthy volunteers.

Model Scaling to Children

One additional aim of this work was to predict the pharmacokinetics of paediatric patients based on the adult model. GEOM for simulated peak levels in infants, toddlers, children and adolescents were 12.5 mg/l (95% CI: 11.0; 14.7), 17.4 mg/l (95% CI: 15.5; 20.3), 15.9 mg/l (95% CI: 14.0; 18.8) and 13.6 mg/l (95% CI: 11.8; 16.7). The prediction of PK-Sim® correlated well with observed data of paediatric patients in literature. Published GEOM peak levels were 11.1 mg/l (95% CI: 8.8; 13.9) for premature infants [44], 17.2 mg/l (95% CI: 14.6; 20.4) for toddlers [45], 15.6 mg/l (95% CI: 12.1; 20.1) for children and 12.9 mg/l (95% CI: 9.9; 16.9) for adolescents [11]. In the simulation, peak levels decreased by 15% with increasing body weight about 10 kg in paediatric patients (Fig. 4a). In contrast, trough levels were constant in all investigated virtual paediatric patients and did not correlate to body weight or another covariate (Fig. 4b). This was also valid for the AUC_{0-24h} (Fig. 4c). Simulated GEOM for the AUC_{0-24h} were 108 mg*h/l (95% CI: 79; 162), 116 mg*h/l (95% CI: 82; 179) and 115 mg*h/l (95% CI: 82; 188) and published GEOM were 130 mg*h/l (95% CI: 107; 158) [45], 115 mg*h/l and 117 mg*h/l [11] for toddlers, children and adolescents. Values of the clearance were consistent for all age groups and were also independent of covariates (Fig. 4d). For toddlers, children and adolescents the GEOM of clearance was 7.7 ml/min/m^2 (95% CI: 5.0; 10.6), 7.2 ml/min/m^2 (95% CI: 4.7; 10.1) and 6.8 ml/min/m^2 (95% CI: 4.2; 9.6). Taken together, the model was able to predict the pharmacokinetic of CAS in paediatric patients based on published data of paediatric clinical trials.

DISCUSSION

In order to provide a basis for further clinical investigations of CAS therapy and dosing in paediatric patients, a PBPK model was built and evaluated with raw data from adult patients and scaled to paediatric patients. The simulated data of the final model were in accordance with the observed data of adults in the CASLAMB trial as well as with the observed raw data of adults in the validation dataset (CASMTD trial). Peak levels seem to be underestimated in both trials. In comparison to POP-PK models of the CASLAMB [46] and CASMTD trial [19], all pharmacokinetic parameters as peak

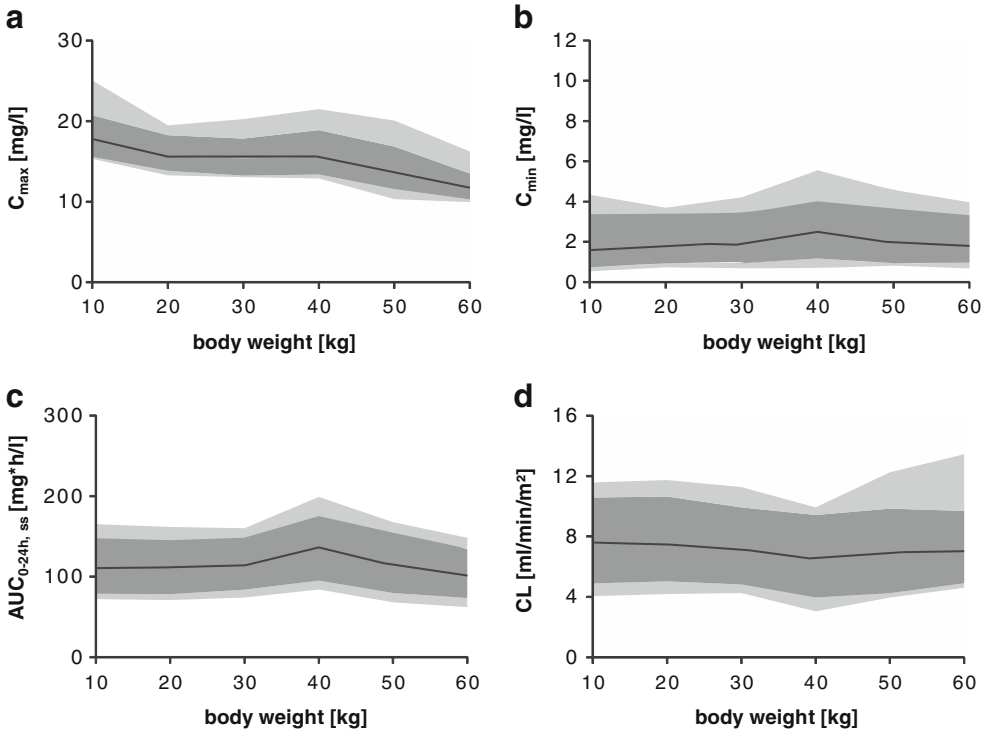

Fig. 4 Correlation between pharmacokinetic parameters peak levels (C_{max}, **a**), through levels (C_{min}, **b**), $AUC_{0–24h}$ (**c**), clearance (CL, **d**) and body weight in virtual paediatric patients. All kinetic parameters were analysed in steady state. *Black line* is the GEOM of the virtual populations, the *dark grey* shaded area is the 95% confidence interval and the *light grey* shaded area is the minimum and maximum. Every population consisted of 100 virtual individuals. Doses were 50 mg/m^2.

levels, trough levels or the $AUC_{0–24h}$ correlate well between POP-PK and PBPK. The GOF plots showed the same correlation between the PBPK model and the observed data as with the POP-PK models [19, 46].

In this analysis, the simulated data of CAS exhibits linear pharmacokinetics. Concentration time curves were superimposable and there was no detectable nonlinearity for protein binding. Peak levels, trough levels and the $AUC_{0–24h}$ were dose depended and in addition clearance, half-life, time to reach steady state and the accumulation of trough levels were independent of doses. This is in accordance with the POP-PK model of the CASMTD trial [19], but in contrast to Migoya *et al.* [15], where time to reach steady state and the accumulation of trough levels did not depend on the dose levels. However, Migoya *et al.* analysed the data by noncompartmental methods and they only suggest a tendency of nonlinear kinetics [15]. Nevertheless, the dose escalation in the CASMTD trial enrolled a limited number of patients and did not consider the γ-phase as there was no measurement later than 24 h after the infusion started, and tissue concentrations were not analysed. Tissue concentrations, especially those in the liver, would be quite interesting, because the modest saturation of OATP1B1 could lead to nonlinear pharmacokinetic of CAS.

Hypothetically, the cause for the interaction of CAS and CsA could be the inhibition of OATP1B1 by CsA [20, 41, 42]. The model in this work was built with the raw data of CASLAMB patients receiving CsA in combination with CAS. The parameterised k_{cat} values of OATP1B1 were compared between CASLAMB patients (with CsA) and CASMTD patients (without CsA). There was no difference between the median k_{cat} of CASLAMB (13.1 min^{-1}) and CASMTD (11.7 min^{-1}). Of note, the trough levels on day 1 of CASLAMB patients and patients receiving the same dose in the CASMTD trial were exactly the same. The parameterisation is conducted by using trough levels. In comparison to healthy virtual individuals, transport is reduced by about 40% in the CASLAMB and CASMTD patients. It is well known that trough levels are higher in patients than in healthy subjects [47]. Taken together, we found no evidence of OATP1B1 being the reason for the interaction between CsA and CAS, which is in contrast to another recent investigation [41]. The difference in the CAS clearance in the clinical studies CASLAMB and CASMTD with and without co-medication of CsA is not very pronounced (0.462 *vs.* 0.411 L/h; [19, 46]). We found an apparent difference between healthy virtual individuals and patients, indicating that disease state might be a factor that influences k_{cat}. However, this hypothesis needs to be further investigated. Clinically, PBPK models need many reliable data from *in-vitro* experiments on transporters and enzymes [23] and there are no available K_M and V_{max} values of OATP1B1 for the transport of CAS in the literature. Hence, it is necessary to analyse V_{max} and K_M *in-vitro* to build a refined PBPK model for CAS.

An important aim of this work was to predict the pharmacokinetics of CAS in paediatric patients. There is a paucity of knowledge, especially in infants and toddlers, and PK data of caspofungin in children are based on small sample sizes. In

comparison to the values in the literature, the simulation was able to predict the pharmacokinetics sufficiently. Of note, there was an apparent correlation between body weight and peak levels, which is in accordance to Li *et al.* [48].

CONCLUSION

Taken together, using clinical trial data in patients, it was possible to build a predictive PBPK model for the antifungal agent CAS. As demonstrated in principle for paediatric patients, the model can be useful for the prediction of the pharmacokinetics in various special populations. In the future, the model could be used as a basis for further clinical investigations in infants and small children. It was able to predict the published concentration-time profiles of children and adolescents [11] correctly. Further investigations should focus on the influence of disease state on the pharmacokinetics of CAS.

ACKNOWLEDGMENTS AND DISCLOSURES

This work was supported by a free software licence of PK-Sim® provided by Bayer Technology Services GmbH, Leverkusen, Germany. AHG has received grants from Gilead and Merck, Sharp & Dohme, is a consultant to Astellas, Gilead, Merck, Sharp & Dohme and Schering-Plough and has served on the speakers' bureaus of Astellas, Gliead, Merck, Sharpe & Dohme, Pfizer, Schering-Plough and Zeneus/Cephalon. JJV is supported by the German Federal Ministry of Research and Education (BMBF grant 01KI0771) and the German Centre for Infection Research. JJV has received research grants from Astellas, Gilead Sciences, Infectopharm, Merck, Pfizer, and Essex/Schering-Plough; and served on the speakers' bureau of Astellas, Merck Sharp Dohme/Merck, Gilead Sciences, Pfizer, and Essex/Schering-Plough. OAC is supported by the German Federal Ministry of Research and Education (BMBF grant 01KN1106), has received research grants from 3 M, Actelion, Astellas, Basilea, Bayer, Celgene, Cubist, Genzyme, Gilead, GSK, Merck/MSD, Miltenyi, Optimer, Pfizer, Quintiles, and Viropharma, is a consultant to 3 M, Astellas, Basilea, Cubist, Da Volterra, Daiichi Sankyo, F2G, Gilead, GSK, Merck/MSD, Optimer, Pfizer, Sanofi Pasteur and Summit/Vifor, and received lecture honoraria from Astellas, Gilead, Merck/MSD, and Pfizer. GH receives research grants from Bayer Technology Services GmbH, Leverkusen, Germany.

REFERENCES

1. Maertens J, Raad I, Petrikkos G, Boogaerts M, Selleslag D, Petersen FB, *et al.* Efficacy and safety of caspofungin for treatment of invasive aspergillosis in patients refractory to or intolerant of conventional antifungal therapy. Clin Infect Dis. 2004;39(11):1563–71.
2. Mora-Duarte J, Betts R, Rotstein C, Colombo AL, Thompson-Moya L, Smietana J, *et al.* Comparison of caspofungin and amphotericin B for invasive candidiasis. N Engl J Med. 2002;347(25):2020–9.
3. Villanueva A, Arathoon EG, Gotuzzo E, Berman RS, DiNubile MJ, Sable CA. A randomized double-blind study of caspofungin *versus* amphotericin for the treatment of candidal esophagitis. Clin Infect Dis. 2001;33(9):1529–35.
4. Villanueva A, Gotuzzo E, Arathoon EG, Noriega LM, Kartsonis NA, Lupinacci RJ, *et al.* A randomized double-blind study of caspofungin *versus* fluconazole for the treatment of esophageal candidiasis. Am J Med. 2002;113(4):294–9.
5. Arathoon EG, Gotuzzo E, Noriega LM, Berman RS, DiNubile MJ, Sable CA. Randomized, double-blind, multicenter study of caspofungin *versus* amphotericin B for treatment of oropharyngeal and esophageal candidiases. Antimicrob Agents Chemother. 2002;46(2):451–7.
6. Sable C, Nguyen B, Chodakewitz J, DiNubile M. Safety and tolerability of caspofungin acetate in the treatment of fungal infections. Transpl Infect Dis. 2002;4(1):25–30.
7. Sawistowska-Schroeder ET, Kerridge D, Perry H. Echinocandin inhibition of 1, 3-β-D-glucan synthase from *Candida albicans*. FEBS Lett. 1984;173(1):134–8.
8. Shematek EM, Braatz JA, Cabib E. Biosynthesis of the yeast cell wall. I. Preparation and properties of beta-(1 leads to 3) glucan synthetase. J Biol Chem. 1980;255(3):888–94.
9. Kurtz M, Heath I, Marrinan J, Dreikorn S, Onishi J, Douglas C. Morphological effects of lipopeptides against *Aspergillus fumigatus* correlate with activities against (1, 3)-beta-D-glucan synthase. Antimicrob Agents Chemother. 1994;38(7):1480–9.
10. MSD. Package insert of Caspofungin. 2011.
11. Walsh TJ, Adamson PC, Seibel NL, Flynn PM, Neely MN, Schwartz C, *et al.* Pharmacokinetics, safety, and tolerability of caspofungin in children and adolescents. Antimicrob Agents Chemother. 2005;49(11):4536–45.
12. Hajdu R, Thompson R, Sundelof JG, Pelak BA, Bouffard FA, Dropinski JF, *et al.* Preliminary animal pharmacokinetics of the parenteral antifungal agent MK-0991 (L-743,872). Antimicrob Agents Chemother. 1997;41(11):2339–44.
13. Stone JA, Xu X, Winchell GA, Deutsch PJ, Pearson PG, Migoya EM, *et al.* Disposition of caspofungin: role of distribution in determining pharmacokinetics in plasma. Antimicrob Agents Chemother. 2004;48(3):815–23.
14. Stone EA, Fung HB, Kirschenbaum HL. Caspofungin: an echinocandin antifungal agent. Clin Ther. 2002;24(3):351–77.
15. Migoya EM, Mistry GC, Stone JA, Comisar W, Sun P, Norcross A, *et al.* Safety and pharmacokinetics of higher doses of caspofungin in healthy adult participants. J Clin Pharmacol. 2011;51(2):202–11.
16. Sandhu P, Lee W, Xu X, Leake BF, Yamazaki M, Stone JA, *et al.* Hepatic uptake of the novel antifungal agent caspofungin. Drug Metab Dispos. 2005;33(5):676–82.
17. Balani SK, Xu X, Arison BH, Silva MV, Gries A, DeLuna FA, *et al.* Metabolites of caspofungin acetate, a potent antifungal agent, in human plasma and urine. Drug Metab Dispos. 2000;28(11):1274–8.
18. Stone JA, Holland SD, Wickersham PJ, Sterrett A, Schwartz M, Bonfiglio C, *et al.* Single- and multiple-dose pharmacokinetics of caspofungin in healthy men. Antimicrob Agents Chemother. 2002;46(3):739–45.
19. Wuerthwein G, Cornely OA, Trame MN, Vehreschild JJ, Vehreschild MJ, Farowski F, *et al.* Population pharmacokinetics of escalating doses of caspofungin in a phase II study of patients with invasive aspergillosis. Antimicrob Agents Chemother. 2013;57(4):1664–71.
20. Ullmann AJ. Review of the safety, tolerability, and drug interactions of the new antifungal agents caspofungin and voriconazole. Curr Med Res Opin. 2003;19(4):263–71.

21. Schmitt W, Willmann S. Physiology-based pharmacokinetic modeling: ready to be used. Drug Discov Today : Technol. 2004;1(4):449–56.
22. Khalil F, Laer S. Physiologically based pharmacokinetic modeling: methodology, applications, and limitations with a focus on its role in pediatric drug development. J Biomed Biotechnol. 2011;2011:1–13.
23. Edginton AN, Theil F-P, Schmitt W, Willmann S. Whole body physiologically-based pharmacokinetic models: their use in clinical drug development. Expert Opin Drug Metab Toxicol. 2008;4(9):1143–52.
24. Espie P, Tytgat D, Sargentini-Maier ML, Poggesi I, Watelet JB. Physiologically based pharmacokinetics (PBPK). Drug Metab Rev. 2009;41(3):391–407.
25. von Kleist M, Huisinga W. Physiologically based pharmacokinetic modelling: a sub-compartmentalized model of tissue distribution. J Pharmacokinet Pharmacodyn. 2007;34(6):789–806.
26. Jones HM, Parrott N, Jorga K, Lavé T. A novel strategy for physiologically based predictions of human pharmacokinetics. Clin Pharmacokinet. 2006;45(5):511–42.
27. Edginton AN, Schmitt W, Voith B, Willmann S. A mechanistic approach for the scaling of clearance in children. Clin Pharmacokinet. 2006;45(7):683–704.
28. Groll AH, Silling G, Young C, Schwerdtfeger R, Ostermann H, Heinz WJ, *et al.* Randomized comparison of safety and pharmacokinetics of caspofungin, liposomal amphotericin B, and the combination of both in allogeneic hematopoietic stem cell recipients. Antimicrob Agents Chemother. 2010;54(10):4143–9.
29. Cornely OA, Vehreschild JJ, Vehreschild MJ, Wuerthwein G, Arenz D, Schwartz S, *et al.* Phase II dose escalation study of caspofungin for invasive aspergillosis. Antimicrob Agents Chemother. 2011;55(12):5798–803.
30. MSD. http://www.cancias.de. 07.09.2013.
31. Nishimura M, Naito S. Tissue-specific mRNA expression profiles of human ATP-binding cassette and solute carrier transporter superfamilies. Drug Metab Pharmacokinet. 2005;20(6):452–77.
32. Morrissey K, Wen C, Johns S, Zhang L, Huang S, Giacomini K. The UCSF-FDA TransPortal: a public drug transporter database. Clin Pharmacol Ther. 2012;92(5):545–6.
33. Nakanishi T, Tamai I. Genetic polymorphisms of OATP transporters and their impact on intestinal absorption and hepatic disposition of drugs. Drug Metab Pharmacokinet. 2012;27(1):106–21.
34. Niemi M, Pasanen MK, Neuvonen PJ. Organic anion transporting polypeptide 1B1: a genetically polymorphic transporter of major importance for hepatic drug uptake. Pharmacol Rev. 2011;63(1):157–81.
35. Krauss M, Burghaus R, Lippert J, Niemi M, Neuvonen P, Schuppert A, *et al.* Using bayesian-PBPK modeling for assessment of inter-individual variability and subgroup stratification. In Silico Pharmacol. 2013;1(1):1–11.
36. Rodgers T, Leahy D, Rowland M. Physiologically based pharmacokinetic modeling 1: predicting the tissue distribution of moderate-to-strong bases. J Pharm Sci. 2005;94(6):1259–76.
37. Rodgers T, Rowland M. Physiologically based pharmacokinetic modelling 2: predicting the tissue distribution of acids, very weak bases, neutrals and zwitterions. J Pharm Sci. 2006;95(6):1238–57.
38. Valentin J. Basic anatomical and physiological data for use in radiological protection: reference values: ICRP Publication 89. Ann ICRP. 2002;32(3):1–277.
39. McNamara PJ, Alcorn J. Protein binding predictions in infants. AAPS Pharm Sci. 2002;4(1):19–26.
40. Rubin MI, Bruck E, Rapoport M, Snively M, McKay H, Baumler A. Maturation of renal function in childhood: clearance studies. J Clin Investig. 1949;28(5):1144–62.
41. Gertz M, Cartwright CM, Hobbs MJ, Kenworthy KE, Rowland M, Houston JB, *et al.* Cyclosporine inhibition of hepatic and intestinal CYP3A4, uptake and efflux transporters: application of PBPK modeling in the assessment of drug-drug interaction potential. Pharm Res. 2013;30(3):761–80.
42. Amundsen R, Christensen H, Zabihyan B, Asberg A. Cyclosporine A, but not tacrolimus, shows relevant inhibition of organic anion-transporting protein 1B1-mediated transport of atorvastatin. Drug Metab Dispos. 2010;38(9):1499–504.
43. Hornik K. The R, project. 2014.
44. Saez-Llorens X, Macias M, Maiya P, Pineros J, Jafri HS, Chatterjee A, *et al.* Pharmacokinetics and safety of caspofungin in neonates and infants less than 3 months of age. Antimicrob Agents Chemother. 2009;53(3):869–75.
45. Neely M, Jafri HS, Seibel N, Knapp K, Adamson PC, Bradshaw SK, *et al.* Pharmacokinetics and safety of caspofungin in older infants and toddlers. Antimicrob Agents Chemother. 2009;53(4):1450–6.
46. Wuerthwein G, Young C, Lanvers-Kaminsky C, Hempel G, Trame MN, Schwerdtfeger R, *et al.* Population pharmacokinetics of liposomal amphotericin B and caspofungin in allogeneic hematopoietic stem cell recipients. Antimicrob Agents Chemother. 2012;56(1):536–43.
47. Nguyen TH, Hoppe-Tichy T, Geiss HK, Rastall AC, Swoboda S, Schmidt J, *et al.* Factors influencing caspofungin plasma concentrations in patients of a surgical intensive care unit. J Antimicrob Chemother. 2007;60(1):100–6.
48. Li CC, Sun P, Dong Y, Bi S, Desai R, Dockendorf MF, *et al.* Population pharmacokinetics and pharmacodynamics of caspofungin in pediatric patients. Antimicrob Agents Chemother. 2011;55(5):2098–105.